Poly(2,7-phenanthrylene)s and Poly(3,6-phenanthrylene)s as Polyphenylene and Poly(phenylenevinylene) Analogues

Changduk Yang,[†] Horst Scheiber,[‡] Emil J. W. List,[‡] Josemon Jacob,[†] and Klaus Müllen*,[†]

Max-Planck-Institut für Polymerforschung, Ackermannweg 10, D-55128 Mainz, Germany, Christian Doppler Laboratory "Advanced Functional Materials", Institute of Solid State Physics, Graz University of Technology, Petersgasse 16, A-8010 Graz, Austria, and Institute of Nanostructured Materials and Photonics, Joanneum Research, Franz-Pichler-Strasse 30, A-8160 Weiz, Austria

Received May 5, 2006; Revised Manuscript Received May 27, 2006

ABSTRACT: The synthesis of a series of soluble poly(2,7-phenanthrylene)s and poly(3,6-phenanthrylene)s is presented. Depending on the nature of the repeat units they constitute analogues of poly(*p*-phenylene) (PPP) and poly(*p*-phenylenevinylene) (PPV) and thus should give rise to different modes of extended π-conjugation. In the case of the 9,10-dialkyl-substituted poly(2,7-phenanthrylene) and poly(3,6-phenanthrylene), spectroscopic characterization suggests polymer aggregation in the solid state, which can be efficiently suppressed by the introduction of aryl substituents to result in a narrow blue emission. The 2,7- or 3,6-coupling of the phenanthrenes has a strong influence on the emission properties of the polymers. The PPP analogue shows less vibronic coupling in emission due to the rigid-rod nature of the polymer as compared to the PPV analogue. Moreover, the photoinduced absorption features of the 2,7-linked derivatives are similar to PPP-type polymers, whereas the 3,6-linked derivatives exhibit a behavior typically found in PPV-type polymers. In the solid state, the PPV analogues show a more pronounced red-shift of the emission, which is assigned to the solid-state packing of the polymers. The polymers display deep blue electroluminescence and good color stability when tested in a polymer light emitting device. The formation of long wavelength emission bands, typically attributed to keto defects, is not observed. Additionally, 2,7- and 3,6-linked tris(phenanthrylene)s are synthesized as model compounds and their optical properties discussed in comparison with their polymer analogues.

Introduction

Recent research into polymer-based organic light-emitting diodes (OLEDs) has focused on the use of conjugated polymers, such as poly(*p*-phenylenevinylene)s (PPVs) and poly(*p*-phenylene)s (PPPs), owing to their high photoluminescence efficiency in thin films. PPV (**P1**) and its derivatives have several advantages as emitting materials such as high thermal stability, good film forming ability, and suitable color tunability (Figure 1).[1−6] To get full-color displays, efficient red, green, and blue-emitting materials are required. Of these, the last has proved to be the most difficult, with a major focus of investigation on materials derived from PPP. PPP (**P2**) and its derivatives constitute a particularly important class since they emit in the blue[7−9] and are suitable hosts for upconversion emission, which is significant for the development of blue lasers.[10,11] However, the PPP backbone has a 23° twist between consecutive phenylene units due to ortho-hydrogen interactions.[12,13] Introduction of solubilizing side chains leads to steric interactions, which cause a marked increase in the phenylene−phenylene torsional angles, with a concurrent loss of π-overlap and a significant blue-shift in the emission wavelength.[14−16] To overcome this, totally planarized ladder-type PPP (LPPPs, **P3**)[17] and the so-called angular poly(acene)s, **P4**,[18,19] have been developed. These materials, however, show blue-green emission in solution (λ_{em} = 450−470 nm for **P3** and λ_{em} = 478−516 nm for **P4**) and tend to form aggregates. As a result, considerable attention has been paid to stepladder polymers in which the PPP backbone is only partially planarized by methine-bridges such as poly(dialkylfluorene)s (PFs, **P5**)[20−22] and poly(tetraalkylindenofluorene)s (PIFs, **P6**).[23,24] These materials exhibit efficient blue emission in solution from 420 to 450 nm with the emission color red-shifting with increasing chain rigidity. However, the blue emission of these derivatives in the solid state appears to be unstable due to the rapid appearance of long-wavelength emission bands (Figure 1).

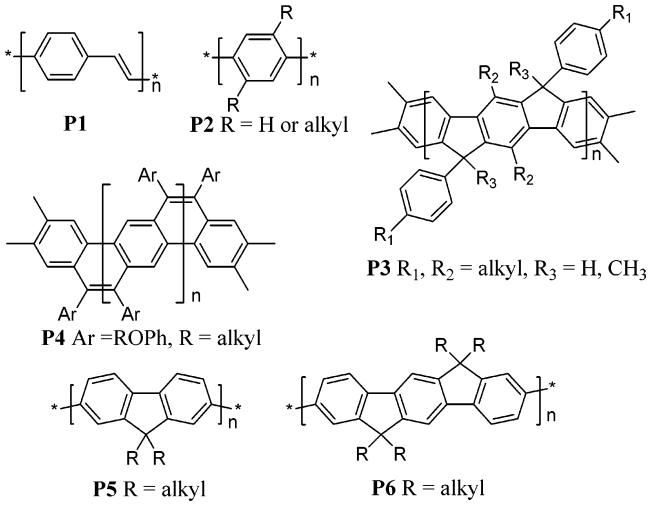

Figure 1. Structures of phenylene-based polymers.

A stepladder polymer containing the phenanthrylene moiety can offer three major advantages: (1) the attachment of alkyl or aryl solubilizing groups at the 9,10-positions enhances solubility without disturbing the conjugation along the chain;

* Corresponding author. Telephone: +49 6131 379 150. Fax: +49 6131 379 350. E-mail: muellen@mpip-mainz.mpg.de.
[†] Max-Planck-Institut für Polymerforschung.
[‡] Graz University of Technology and Institute of Nanostructured Materials and Photonics.

10.1021/ma061007p CCC: $33.50
Published on Web 07/14/2006

Chart 1. Synthetic Protocols for the Preparation of the Polyphenanthrylenes and the Structures as (a) PPP Analogue and (b) PPV Analogue[a]

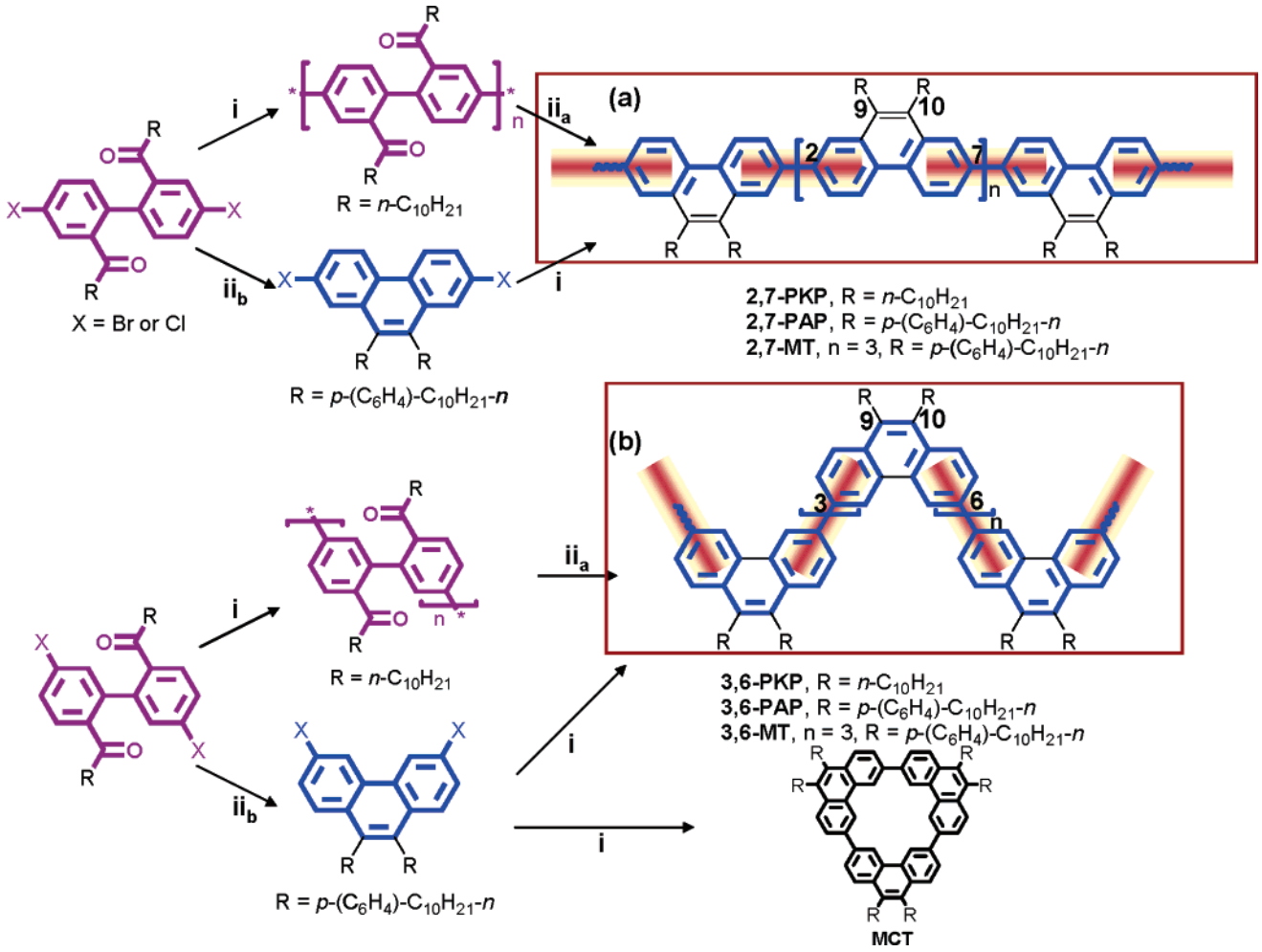

[a] Key: (i) Nickel(0)-mediated Yamamoto-type polycondensation; (ii$_a$) Polymer-analogous cyclization by McMurry-type coupling; (ii$_b$) cyclization with B_2S_3 generated in situ

(2) the partial planarization of the π-system in the aromatic repeat unit leads to an emission in the pure blue region of the electromagnetic spectrum, compared to the emission from the parent PPP (**P2**); (3) the interruption of the planarity within the stepladder polymers would reduce the unwanted low energy emission band, which has been observed for LPPP-based OLEDs.

In addressing these advantages, we direct our attention toward the synthesis of phenanthrylene-based polymers for a blue emitter in OLEDs, which to the best of our knowledge, only one patent has described a similar approach for the synthesis of poly(2,7-phenanthrylene)s[25] We describe here the synthesis and detailed characterization of a series of novel polyphenanthrylenes, which can be viewed either as PPP or PPV analogues. Phenanthrylenes can be polymerized from either a 2,7-substituted monomer to generate a linear, rodlike PPP-type chain or from a 3,6-substituted monomer to create a kinked PPV-analogue (Chart 1). Additionally, the synthesis of 2,7- and 3,6-linked tris(phenanthrylene)s (**2,7-MT** and **3,6-MT**), which serve as model compounds for the spectroscopic characterization of the corresponding polymers, is described.

Two synthetic approaches were utilized to generate the target polymers (Chart 1): (i) by a nickel(0)-mediated Yamamoto-type coupling of 2,7- or 3,6-dihalophenanthrene monomers and (ii) by initial polymerization of a diketone precursor monomer and subsequent polymer-analogous ring closure. Notably, while a Yamamoto-type polycondensation of 3,6-dihalophenanthrenes predominantly leads to the formation of a macrocyclic trimer **MCT** (Chart 1), a Suzuki−Miyaura-type polycondensation can afford PPV-type polyphenanthrylenes with improved molecular weights due to the avoidance of the formation of **MCT**.

Results and Discussion

The synthetic approach to poly(2,7-(9,10-dialkylphenanthrylene)) is depicted in Scheme 1. 2,5-Dibromobenzoic acid was first converted to the 2,5-dibromobenzoyl chloride by treatment with oxalyl chloride, which was then coupled with decyllithium in the presence of copper(I) cyanide to generate 2′,5′-dibromo-undecylphenone (**1**) in 70% isolated yield.[13] Ullmann coupling of **1** in the presence of copper powder gave 4,4′-dibromo-2,2′-di(undecyloyl)-1,1′-biphenyl (**2**) (43%). Reductive cyclization of this compound using either tricyclohexyltin sulfide and trichloroborane, or with hydrazine in a polar solvent (acetic acid) by a modified Wolff−Kishner reaction, was not successful. Although McMurry-type coupling with $TiCl_3/LiAlH_4$ led to ring closure of **2**,[26] simultaneous debromination was also observed. Hence, the target polymer **2,7-PKP** was prepared by initial polymerization of **2** and subsequent polymer-analogous McMurry coupling. The biphenyl polymer **3** was synthesized by a nickel(0)-mediated Yamamoto-type polycondensation. It is readily soluble in organic solvents like THF, toluene, chloroform, and dichloromethane (M_n = 2.32 ×

Scheme 1. Synthesis of Poly(2,7-(9,10-dialkylphenanthrylene))

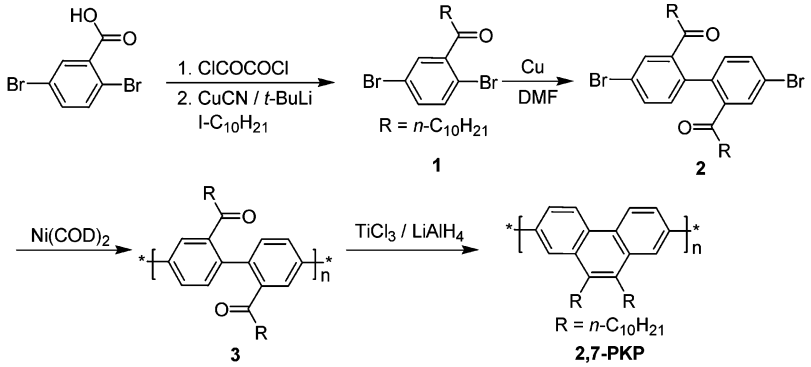

Scheme 2. Synthesis of Poly(3,6-(9,10-dialkylphenanthrylene))

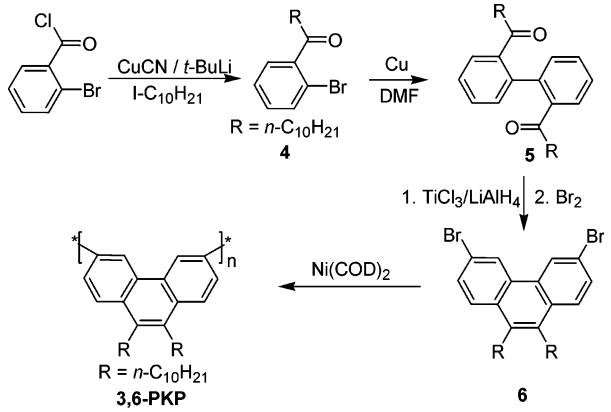

10^4 g/mol, $M_w = 4.25 \times 10^4$ g/mol, THF, PPP standards). Following cyclization of **3**, the target polymer **2,7-PKP** possesses an M_n of 4.68×10^4 g/mol and M_w of 9.78×10^4 g/mol as determined by gel-permeation chromatography (GPC) analysis against PPP standards.[27] To confirm that the polymer-analogous ring closure had gone to completion, the polymers were characterized by FT-IR and ^{13}C NMR spectroscopy. The strong peak at 1690 cm^{-1} in the FT-IR spectrum of **3**, which is assignable to the carbonyl group, is not observed in the spectrum of **2,7-PKP**.[28] An inspection of the ^{13}C NMR spectrum of **2,7-PKP** fails to reveal any carbonyl signals which would point toward the presence of uncyclized precursor **3**. In view of the signal-to-noise ratio achieved we can conclude that the amount of structural defects is below 1%. This polymer has limited solubility in common organic solvents (THF, toluene, dichloromethane, etc.).

The analogous 3,6-linked polymer **3,6-PKP** was synthesized starting from 2-bromobenzoyl chloride as shown in Scheme 2. The synthetic sequences are similar to the one described earlier (acylation, Ullmann, and McMurry) and the dibromide monomer **6** was isolated in an overall yield of 38%. The yield-limiting step in the synthesis is the bromination of the phenanthrene moiety. To avoid overbromination, which resulted in an inseparable mixture of di-, tri- and tetra(bromophenanthrene)s, less than 2 equiv of bromine was added to the reaction vessel. The desired product **6** could then be isolated from the underbrominated side-products. **3,6-PKP** was synthesized by a Yamamoto-type polycondensation and is readily soluble in organic solvents. GPC analysis of **3,6-PKP** exhibits a M_n value of 3.15×10^3 g/mol and M_w of 5.10×10^3 g/mol (THF, PPP standards). Although attempts were undertaken to improve the molecular weight by varying the monomer concentration as well as the mode of mixing the solutions of the nickel reagent and the monomer,[29] the polymerization always resulted in low molecular weight ($M_n = (3.0-4.0) \times 10^3$ g/mol) materials.

To better understand the reason for the observed low molecular weight of the 3,6-linked system,we proceeded to prepare the corresponding 9,10-diaryl-substituted analogues. Scheme 3 illustrates the synthetic approach toward **3,6-PAP**. 4-Chloro-2-iodo-4′-decylbenzophenone (**7**) was prepared by $AlCl_3$-promoted Friedel−Crafts acylation of decylbenzene with 4-chloro-2-iodobenzoyl chloride in 91% yield. Ullmann-type coupling followed by cyclization of **8** using tricyclohexyltin sulfide and trichloroborane generated **9** in an overall yield of 55%. Although dichloro substitution was believed to be more suitable for Yamamoto-type polymerization[30] than the dibromo case, polymerization of **9** gave only a low molecular weight polymer ($M_n = 3.25 \times 10^3$ g/mol and $M_w = 4.66 \times 10^3$ g/mol, THF, PPP standards). The low molecular weight obtained from the polymerization of **9** can be attributed to the formation of a macrocyclic trimer **MCT** (Chart 1, analogous trimer formation

Scheme 3. Synthesis of Poly(3,6-(9,10-diarylphenanthrylene))

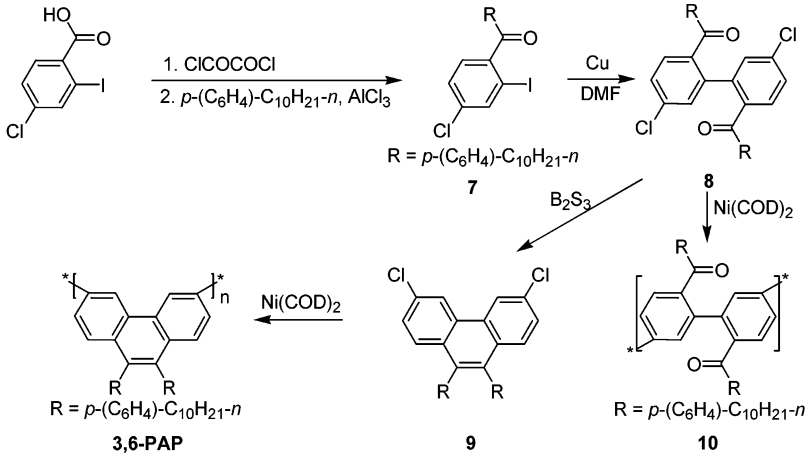

Scheme 4. Synthesis of Linear Poly(3,6-(9,10-diarylphenanthrylene)) via Suzuki Coupling

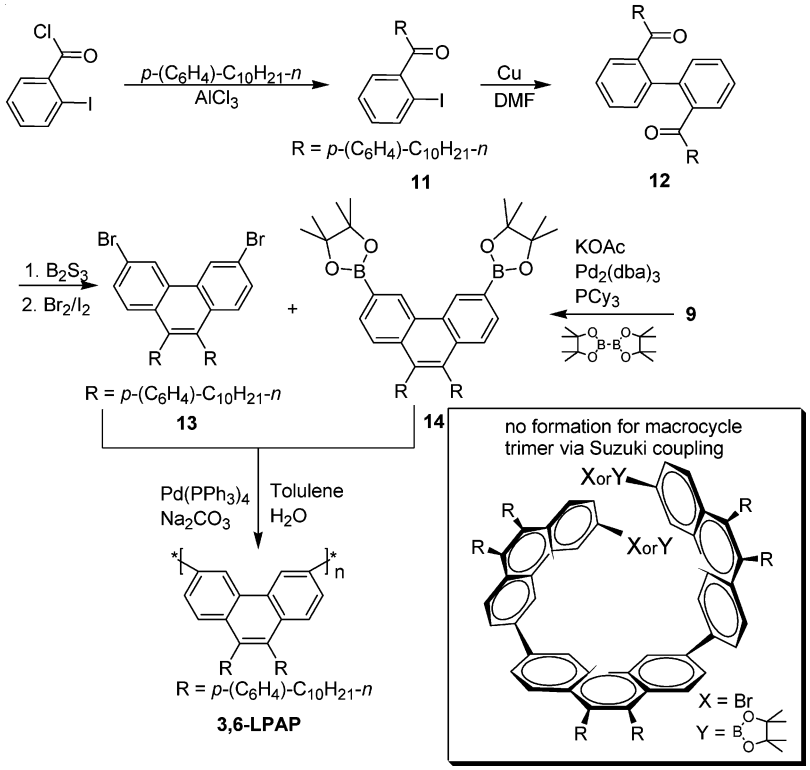

Scheme 5. Synthesis of Poly(2,7-(9,10-diarylphenanthrylene))

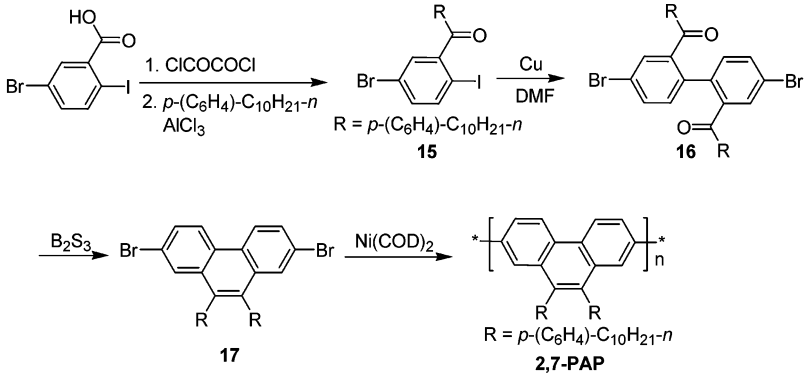

accounts for the low M_n value for **3,6-PKP**). This follows from the intrinsic angle of the phenanthrylene unit which facilitates trimer formation. This was indeed shown by Staab et al., who reported the synthesis of **MCT** (R = H) via the Ullmann coupling of 3,6-diiodophenanthrene.[31] The GPC curve of **3,6-PAP** reveals a large amount of low molecular weight polymer (ca. >2500 g/mol) due to a significant amount of **MCT** in the reaction.[28] **MCT** was further confirmed by independent synthesis, the results of which will be reported separately. The polymerization of precursor **8**, a monomer that does not possess the intrinsic angle due to rotation between the phenyl units of the monomer, did not yield a high molecular weight polymer either ($M_n = 2.14 \times 10^3$ g/mol, THF, PPP standards). Although concrete evidence is lacking at this stage, we attribute this to the possibility of cyclization or the inherent instability of the oxidative addition product formed by the metal complex with **8**.

The preparation of poly(3,6-phenanthrylene) via Suzuki polycondensation was undertaken to improve the molecular weight, because from mechanistic considerations this avoids the formation of **MCT**, as shown in Scheme 4. The 3,6-diboronic ester of phenanthrene **14** was prepared by a palladium-catalyzed coupling reaction of **9** with bis(pinacolato)diboron under $Pd_2(dba)_3/PCy_3$/KOAc and the 3,6-dibromide **13** was synthesized from 2-iodobenzoyl chloride in an approach analogous to that discussed earlier. The Suzuki polycondensation of **13** and **14** gave the linear polymer **3,6-LPAP** with improved molecular weights ($M_n = 5.33 \times 10^3$ g/mol and M_w of 6.82×10^3 g/mol, PPP standards). This polymer has good solubility in common organic solvents.

To complete the series, **2,7-PAP** was synthesized starting from 5-bromo-2-iodobenzoic acid as depicted in Scheme 5 by similar procedures as detailed before. **2,7-PAP** is readily soluble in common solvents ($M_n = 1.13 \times 10^4$ g/mol, $M_w = 5.26 \times 10^4$ g/mol, $D = 4.66$, PPP standards). This high polydispersity index prompted us to have a careful look at the GPC elution curve of **2,7-PAP** which revealed a bimodal molecular weight distribution. We attribute it to low molecular weight oligomeric components which are inseparable by Soxhlet extraction.

TGA thermograms of all the polymers reveal good thermal stability up to 350 °C, which is essential for fabricating stable OLED devices. Weight loss (5%) starts at 380, 425, 445, and 430 °C for polymers **2,7-PKP**, **2,7-PAP**, **3,6-PKP**, and **3,6-LPAP** respectively. DSC analysis of the polymers shows neither

Scheme 6. Synthesis of 2,7-Linked 9,10-Diarylphenanthrylene Trimer

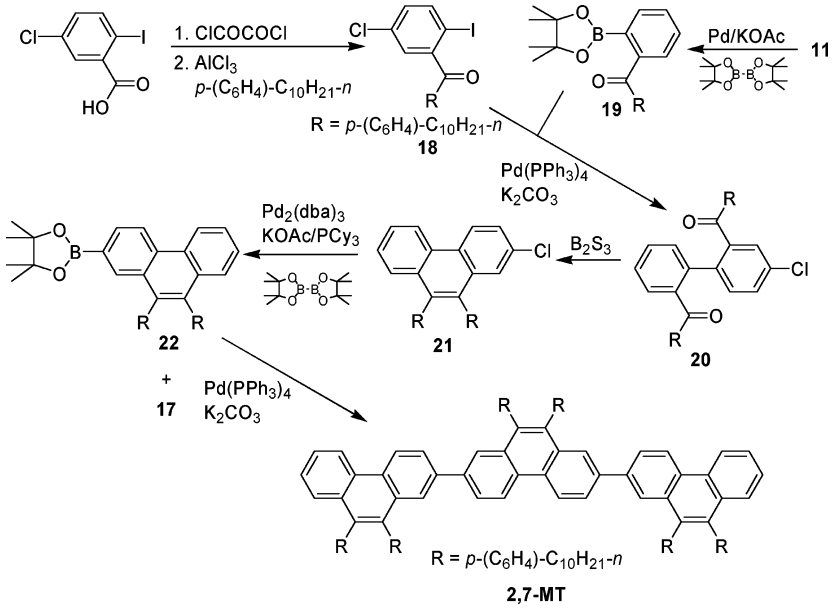

Scheme 7. Synthesis of 3,6-Linked 9,10-Diarylphenanthrylene Trimer

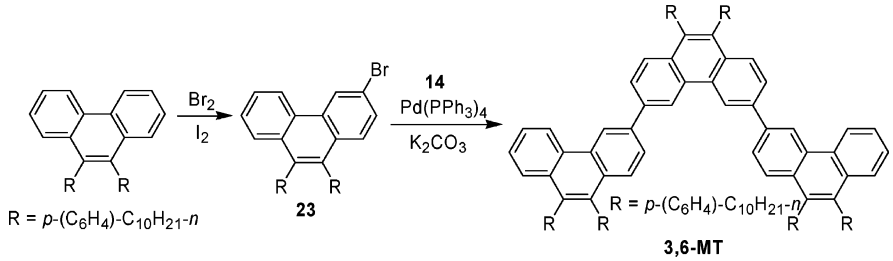

Table 1. Optical and Electrochemical Data of 2,7-PKP, 2,7-PAP, 3,6-PKP, 3,6-LPAP, and the Model Trimers (2,7-MT and 3,6-MT)[b]

	solution λ_{max} (nm)		film λ_{max} (nm)				
compound	absorption	emission	absorption	emission	HOMO (eV)	LUMO (eV)	optical band gap[a] (eV)
2,7-MT	306 (340)	406 (416)					
2,7-PKP	392	448	392	500	−5.56	−2.92	2.84
2,7-PAP	306, 375	400 (424, 451)	381	403(429)	−5.89	−2.81	3.08
3,6-MT	325 (355)	410, 422					
3,6-PKP	343	398, 425 (450)	351	417, 446 (473)	−5.69	−2.59	3.10
3,6-LPAP	343−357	403, 426 (456)	365−378	424 (451)	−5.71	−2.65	3.08

[a] Estimated from a combination of CV data and the onset wavelength of optical absorption in THF solution. [b] Peaks that appear as shoulders or weak bands are shown in parentheses.

a glass transition process (T_g) nor other thermal processes (such as liquid crystalline phase) from −50 to +200 °C.

Synthesis of 2,7- and 3,6-Linked Model Trimers and Their Characterization. To more precisely assess the different modes of π-conjugation between poly(2,7-phenanthrylene)s and poly(3,6-phenanthrylene)s, 2,7- and 3,6-linked model trimers were prepared according to Schemes 6 and 7. 5-Chloro-2-iodo-4′-decylbenzophenone (**18**) was coupled with the boronic ester **19** (50%) by the Suzuki reaction, and subsequent cyclization of **20** gave 2-chloro-9,10-di(4-decyl-phenyl)-phenanthrene (**21**) (89%). Compound **21** was converted to the corresponding boronic ester **22** under $Pd_2(dba)_3$/KOAc with tricyclohexylphosphine as a ligand (72%). Suzuki coupling of **22** with **17** afforded 2,7-linked trimer **2,7-MT** (26%). The synthesis of the 3,6-linked analogue **3,6-MT** was achieved via Suzuki coupling of **23** with **14** (71%).

Electrochemical Properties. The redox behavior of thin films of **2,7-PKP**, **2,7-PAP**, **3,6-PKP**, and **3,6-LPAP** was investigated by cyclic voltammetry (CV) against Ag/Ag+. All polymers show an irreversible oxidation, with oxidation onset values ranging from 1.54 V vs Ag/Ag+ for **3,6-PKP**, 1.57 V for **3,6-LPAP**, 1.61 V for **2,7-PKP**, and 1.64 V for **2,7-PAP**. The CV data listed in Table 1 point toward a slight increase in the oxidation onset of the 2,7-linked polymers (**2,7-PKP** and **2,7-PAP**). Calculating the energy level of Ag/AgCl to be −4.4 eV from the ferrocene/ferrocenium standard,[32,33] and determining the band gap from the absorption onset, the HOMO and LUMO values for **3,6-PKP** are estimated to be −5.55 eV and −2.45 eV, respectively. The corresponding HOMO and LUMO values are −5.71 and −2.65 eV for **3,6-LPAP**, −5.56 and −2.72 eV for **2,7-PKP**, −5.89 and −2.81 eV for **2,7-PAP**, respectively.[20]

Photoluminescence Properties. The UV−vis absorption and photoluminescence properties of all polymers (**2,7-PKP**, **2,7-PAP**, **3,6-PKP**, and **3,6-LPAP**), as well as the model compounds (**2,7-MT** and **3,6-MT**), were investigated in THF solution and in thin films (Figures 2−7). Transparent and uniform polymer films were prepared on quartz by spin-casting from THF or chloroform solutions at room temperature. The absorption and PL emission spectral data for all the materials are summarized in Table 1.

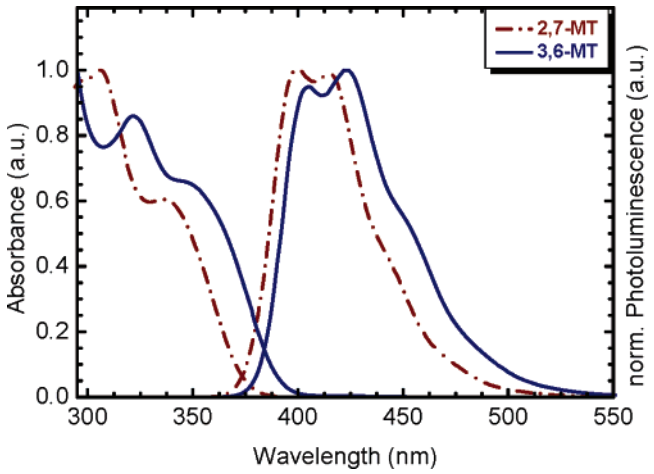

Figure 2. UV−vis absorption and photoluminescence spectra of **2,7-MT** and **3,6-MT** in THF solution.

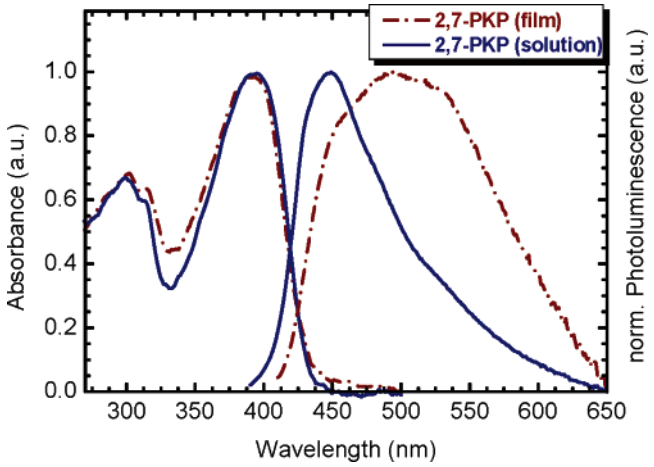

Figure 3. UV−vis absorption and photoluminescence spectra (λ_{exc} = 370 nm) of **2,7-PKP** film and in THF solution.

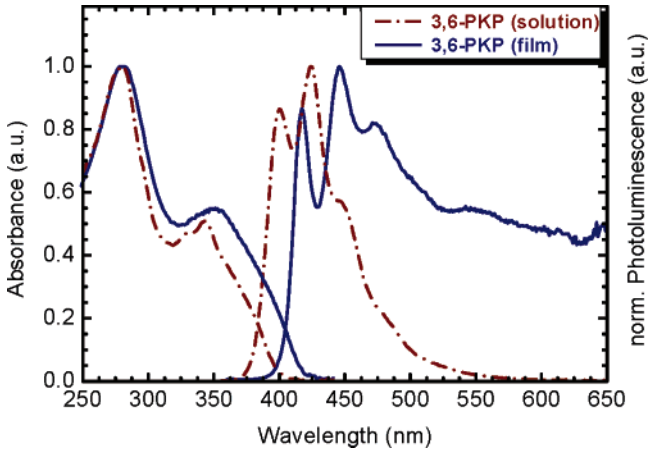

Figure 4. UV−vis absorption and photoluminescence spectra (λ_{exc} = 370 nm) of **3,6-PKP** film and in THF solution.

2,7-MT and 3,6-MT. The absorption spectra of **2,7-MT** and **3,6-MT** in solution are similar in shape. The emission spectra from both compounds show a clear vibronic fine structure with an energetic spacing of ca. 150−160 meV for all transitions. The observation of a systematic bathochromic shift of 50 meV between **2,7-MT** and **3,6-MT** in absorption and emission is a clear indication that the linear PPP-analogue has a reduced π-conjugation when compared to the PPV-analogue, consisting of linked, planarized *cis*-stilbene units.

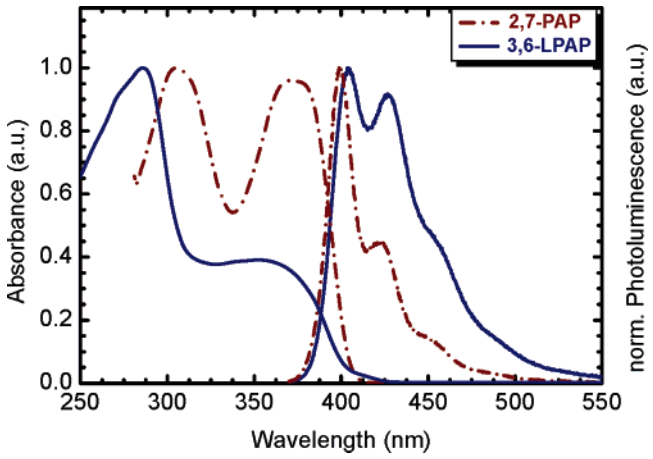

Figure 5. UV−vis absorption and photoluminescence spectra (λ_{exc} = 370 nm) of **2,7-PAP** and **3,6-LPAP** THF in solution.

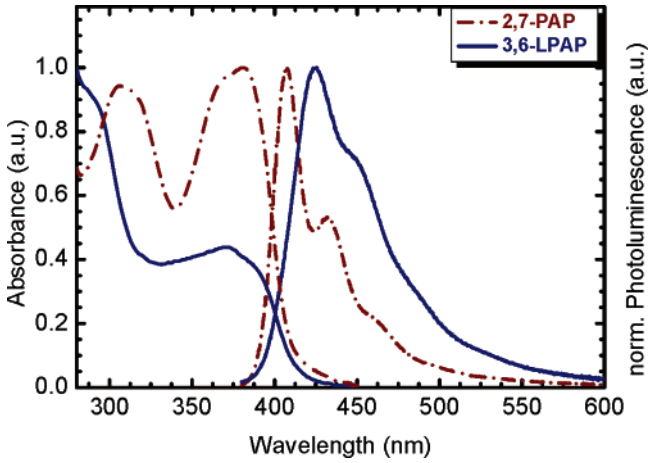

Figure 6. UV−vis absorption and photoluminescence spectra (λ_{exc} = 370 nm) of **2,7-PAP** and **3,6-LPAP** films.

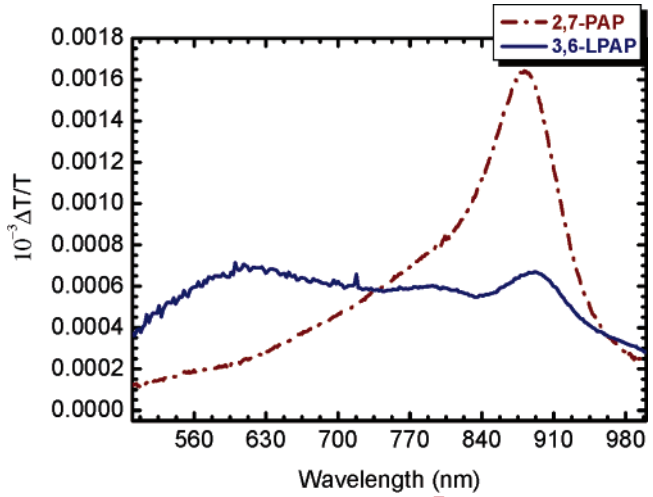

Figure 7. Photoinduced absorption spectra of **2,7-PAP** and **3,6-LPAP** films recorded at 100 K.

2,7-PKP and 3,6-PKP in Solution and as Thin Film. The absorption maxima in solution for **2,7-PKP** and **3,6-PKP** are at 392 and 343 nm respectively, arising from π-π* transitions of the conjugated polymer backbone (Figures 3 and 4). In the film of **2,7-PKP**, a large bathochromic shift of the onset of the emission of ca. 150 meV is observed, with an additional broad, long wavelength emission band. This low energy emission can be due to aggregation or a more planar configuration of the 9,10-dialkyl-substituted phenanthrylene unit, in comparison with

the analogous polymer with 9,10-aryl substituents. Note that this bathochromic shift of the onset of emission between 50 and 150 meV is typical for linear PPP-type polymers[34] as a consequence of the reduced inter-ring twist in the solid state. In the case of **3,6-PKP**, the thin film emission and absorption spectra are similar to those recorded in solution, with a typical bathochromic shift of ca. 130 meV. This compound exhibits a long-wavelength tail emission, starting around 500 nm which can be attributed to aggregation of the phenanthrylene units with alkyl substituents at the 9,10-positions.

2,7-PAP and 3,6-LPAP in Solution and as Thin Film. The poly(9,10-dialkylphenanthrylene)s presented so far, **2,7-PKP** and **3,6-PKP**, show in addition to the observed spectral features broad, long wavelength emission bands in the solid state due to increased interaction of the polymer chains in the solid-state masking the intrinsic molecular properties of the polymers. Therefore, to study the influence of the 2,7- and 3,6-conjugation on the properties of excited states, the corresponding aryl-substituted compounds **2,7-PAP** and **3,6-LPAP** are more revealing because they do not exhibit the long wavelength emission, as a consequence of the suppressed aggregation in the solid state due to increased steric interactions from the aryl groups. In addition to suppressing the unwanted long wavelength emission bands, **2,7-PAP** and **3,6-LPAP** exhibit much better film forming properties, allowing for the ready fabrication of light emitting devices. As depicted in Figure 5, the absorption spectrum of **3,6-LPAP** in THF solution has one distinguishable broader band when compared to that of **2,7-PAP**.

A comparison of the absorption and emission spectra of **2,7-PAP** and **3,6-LPAP** in solution reveals a significant broadening of the bands in **3,6-LPAP**, in addition to a bathochromic shift in the emission spectrum by 10 meV for the PPV-analogue. This is accompanied by a less pronounced 0−0 transition and an increased Huang−Rhys factor. This observation indicates that in the linear 2,7-linked compound there is less vibronic coupling due to the rigid-rod nature of the polymer when compared to the PPV-analogue.

Compared to the absorption and emission spectra observed in THF solution, in the solid state **2,7-PAP** only displays a slight red shift of ca. 45 meV. In contrast to the alkyl-substituted **2,7-PKP**, **2,7-PAP** fails to suggest aggregation in the solid state, as depicted in Figure 6. Conversely, for **3,6-LPAP** the solid-state emission spectrum reveals a more pronounced red shift of ca. 120 meV as compared to the solution spectrum. This observation can indicate that the **3,6-LPAP** possesses a different solid-state packing giving rise to more efficient conjugation along the backbone.

To further elucidate the difference in photoexcited states such as triplet excitons and polarons of **2,7-**PAP and **3,6-LPAP**, the photoinduced absorption (PA) spectra of films have been recorded (Figure 7). **2,7-PAP** displays one dominant band at 880 nm (1.4 eV) with a shoulder at 789 nm (1.6 eV). The 1.4 eV feature has an obvious similarity to the PA spectra of other PPP derivatives,[35,36] such as methyl substituted ladder-type poly(*p*-phenylene) (MeLPPP), where this characteristic was observed at 1.3 eV, with the entire absorption band having a very similar shape. Therefore, this band can be assigned to absorptions within the triplet manifold (T1 → Tn absorption). The high-energy shoulder is also caused by a T1 → Tn absorption, as the lifetime of this absorptive mark is identical to the dominant peak at 1.4 eV. Because of its energetic separation, it is tentatively assigned to a vibronic progression of the absorption. No explicit polaronic absorption is observed.

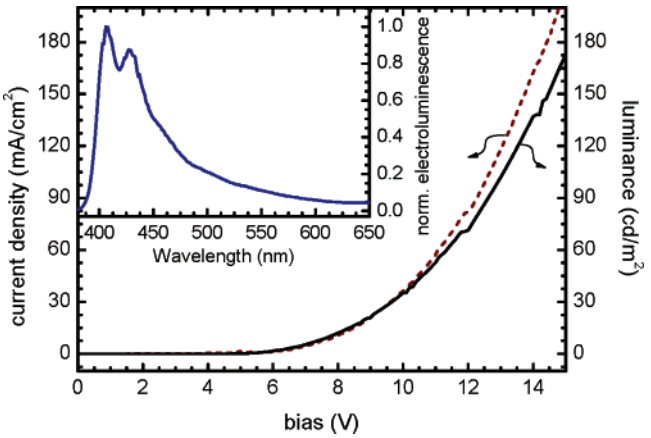

Figure 8. Bias/current and bias/electroluminescence characteristics and normalized electroluminescence of an ITO/PEDOT/**2,7-PAP**/Ca/Al device.

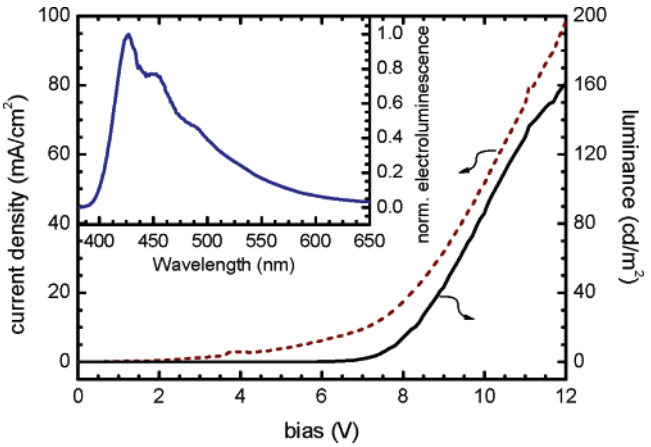

Figure 9. Bias/current and bias/electroluminescence characteristics and normalized electroluminescence of an ITO/PEDOT/**3,6-LPAP**/Ca/Al device.

In contrast, the PA spectrum of **3,6-LPAP** demonstrates a shift of the two T1 → Tn absorption bands to lower energies (785 nm to 892 nm). This is accompanied by a reduction of the signal intensity to about 30% of the signal intensity of **2,7-PAP**. The PA spectrum of **3,6-LPAP** displays a broad band at 615 nm, which is absent in **2,7-PAP**. The observed shift can be explained by the overall lowering of the optical band gap in **3,6-LPAP** as compared to **2,7-PAP**, whereas the additional band at 615 nm is untypical for any PPP-type polymer.[35,36] However, comparing this characteristic of PPV-type polymers, a resemblance to the typically observed broad polaronic absorption can be recognized.[37,38] This again points toward the similarity in the properties of **3,6-LPAP** to PPV-type polymers.

Electroluminescence (EL) Properties. 2,7-PAP and **3,6-LPAP** exhibit the best film forming behavior among the presented polymers and therefore the electroluminescent properties of these two polymers have been tested in a functional device. OLEDs were prepared under an inert atmosphere, with the configuration ITO/PEDOT:PSS/polymer/Ca/Al.

As depicted in Figure 8, OLEDs fabricated from **2,7-PAP** show a deep blue electroluminescence spectrum with a maximum at 403 nm and a spectral shape identical to the thin film PL spectrum. The luminance values are found to be ca. 200 cd/m^2 at a bias voltage of 15 V and color coordinates of the emission are in the deep blue range at $x = 0.19$, $y = 0.14$, according to the CIE standard 1931. The devices display the electroluminescence onset at ca. 4 V in forward bias direction

and exhibit stable blue emission within the first minutes of operation under glovebox conditions and when operated in air. Driving the device at constant current leads to a 50% reduction in luminescence after 10 min, however, without a significant change in the emission spectrum of the device.

OLEDs prepared from **3,6-LPAP** also exhibit an electroluminescence spectrum identical to the PL spectrum in the film, with luminance values of also ca. 200 cd/m^2, however at slightly lower bias voltages of 10 V. The color coordinates are in the deep blue range at $x = 0.18$, $y = 0.16$ according to the CIE standard 1931. These devices are slightly less stable under operation compared to **2,7-PAP** since at constant current over 10 min a 70% reduction in luminescence is observed, but also no spectral degradation of the material is seen during operation under glovebox conditions, as well as under operation in air. These unoptimized single-layer devices show only moderate efficiencies (0.25−0.5 cd/A), indicating that electron-transporting layers or hole blocking layers are required to obtain maximum efficiency in the devices. Investigation into device optimization and detailed investigations on the long-term stability of the polymers are underway and will be reported separately.

Conclusion

In summary, a series of poly(2,7-phenanthrylene)s and poly(3,6-phenanthrylene)s as PPP- and PPV-analogues respectively, have been synthesized by either Yamamoto or Suzuki-type polycondensation. The spectroscopic and electroluminescent properties of the two different types of π-conjugation were compared. The introduction of alkyl or aryl substituents at 9,10-positions of phenanthrene renders these materials soluble and processable. In the case of 2,7-linked polymers it is found that alkyl substituents at 9,10-positions lead to the appearance of an unwanted low energy emission band in the solid state, which is suggestive of aggregation. The introduction of aryl substituents at the 9,10-positions completely suppresses this long wavelength emission, suggesting that the steric bulkiness of the substituents hinders the solid-state packing of the polymers. In the case of 3,6-linked polymers, the Yamamoto polycondensation led to the formation of substantial amounts of a macrocyclic trimer **MCT**. When using a Suzuki-type polycondensation, the formation of **MCT** was mechanistically unfavorable and resulted in improved molecular weight polymers. Both the poly(2,7-phenanthrylene)s and poly(3,6-phenanthrylene)s with aryl substituents display blue emission in solution and film. The PL spectra of **3,6-LPAP** as PPV analogue in both solution and film are bathochromically shifted as compared to the PPP analogous **2,7-PAP**, which can be attributed to the solid-state packing of the polymers. A qualitative comparison of the emission and absorption spectra indicates that the 2,7-linked compounds have less vibronic coupling in emission due to the rigid-rod nature of the polymers when compared to the 3,6-linked compounds. The photoinduced absorption features of **2,7-PAP** are similar to those of PPP-type polymers, whereas the **3,6-LPAP** exhibits characteristics only found in the spectra of PPV-type polymers. **2,7-PAP** and **3,6-LPAP** were incorporated into a single layer OLED as the active emitting material. A peak brightness of the devices of 200 cd/m^2 and good spectral stability is observed while operating under glovebox as well as ambient conditions. Because of the stable blue electroluminescence, both **2,7-PAP** and **3,6-LPAP** are attractive candidates as the emissive materials for OLED-based flat panel display applications. The presented classes of 3,6- and 2,7-conjugated polyphenanthrylenes allow for a unique photophysical investigation, illustrating the PPP-type properties of the 2,7-linked polymers in comparison to the PPV-type properties of the 3,6-linked polymers, thereby further elucidating the structure−property relationships in conjugated polymers.

Experimental Section

General Data. Commercially available materials were used as received unless noted otherwise. ^{1}H and ^{13}C NMR spectra were recorded on a Bruker DPX 250, Bruker AMX 300 or Bruker DRX 500 MHz spectrometer and referenced to the solvent peak. Gel permeation chromatography (GPC) analysis against polystyrene standards was performed in THF on a Waters high pressure GPC assembly with an M590 pump, microStyragel columns of 10^5, 10^4, 10^3, 500, and 100 Å and a refractive index detector. UV−visible absorption spectra were recorded on a Perkin-Elmer Lambda 15 spectrophotometer. Photoluminescence spectra were recorded on a SPEX Fluorolog 2 Type F212 steady-state fluorometer, using a 450 W xenon arc lamp as excitation source and a PMT R 508 photomultiplier as detector system. Thermogravimetric analysis and differential scanning calorimetry (DSC) measurements were carried out on a Mettler 500 thermogravimetric analyzer and Mettler DSC 30 calorimeter, respectively. CV was performed on an EG&G Princeton Applied Research potentiostat, model 270 on 2 μm thick films deposited by solution coating onto precleaned ITO as a working electrode with an area of 0.2 cm^2. After coating, the films were dried in a vacuum oven for 10 min. The measurements were carried out in acetonitrile solutions containing 0.1 M of tetrabutylammonium perchlorate as the supporting electrolyte, using Ag/AgCl as the reference electrode and a platinum wire as the counter electrode and an internal ferrocene/ferrocenium (FOC) standard.

Devices. The ITO covered glass substrates for the OLEDs were thoroughly cleaned in a variety of organic solvents and exposed to an oxygen plasma dry cleaning step. PEDOT:PSS (Baytron P from Bayer Inc.) layers were spin-coating under ambient conditions and dried according to specifications by Bayer Inc. under inert atmosphere. The emissive polymer films were spin-cast from solution and dried at 80 °C overnight in a vacuum. Metal electrodes were thermally deposited in a vacuum coating mounted in a glovebox at a base pressure of below 2×10^{-6} mbar.

EL spectra were recorded using an ORIEL spectrometer with an attached CCD camera. The current/luminance/voltage (ILV) characteristics were recorded in a customized setup using a Keithley 236 source measure unit for recording the current/voltage characteristics while recording the luminance using a calibrated photodiode attached to an integrating sphere (Ulbrich).

Photoinduced Absorption. The samples for PA measurements were prepared by spin-coating on Infrasil substrates. The pump beam was produced by an Ar^+ laser with a laser power of approximately 100 mW, which was mechanically chopped at ~17 Hz, providing the reference for the lock-in amplifier. The sample was mounted in an optically accessible cryostat under a dynamic vacuum of less than 10^{-5} mbar. A 50 W tungsten halogen lamp was the light source for the transmission measurement. All PIA spectra were measured at 100 K and were corrected for PL and the optical throughput of the setup.

Acknowledgment. This work was supported by the Bundesministerium für Bildung und Forschung (Projects 13N8165 OLAS and 13N8215 OLED) and by Dupont Displays. The CDL-AFM is a key member of the long-term AT&S research strategies. C.Yang gratefully acknowledges the Korea Science and Engineering Foundation (KOSEF) for the graduate study abroad scholarship.

Supporting Information Available: Text giving full experimental details for the synthesis of all new materials and figures showing the FT-IR spectra for **3** and **2,7-PKP** and GPC for **3,6-PAP** and **3,6-LPAP**. This material is available free of charge via the Internet at http://pubs.acs.org.

References and Notes

(1) Burroughes, J. H.; Bradley, D. D. C.; Brown, A. R.; Marks, R. N.; Mackay, K.; Friend, R. H.; Burns, P. L.; Holmes, A. B. *Nature (London)* **1990**, *347*, 539−541.
(2) Braun, D.; Heeger, A. J. *Appl. Phys. Lett.* **1991**, *58*, 1982−1984.
(3) Bradley, D. D. C. *Adv. Mater.* **1992**, *4*, 756−758.
(4) Clery, D. *Science* **1994**, *263*, 1700−1702.
(5) Gill, R. E.; Malliaras, G. G.; Wildeman, J.; Hadziioannou, G. *Adv. Mater.* **1994**, *6*, 132−135.
(6) Kraft, A.; Grimsdale, A. C.; Holmes, A. B. *Angew. Chem., Int. Ed.* **1998**, *37*, 402−428.
(7) Grem, G.; Leditzky, G.; Ullrich, B.; Leising, G. *Adv. Mater.* **1992**, *4*, 36−37.
(8) Balanda, P. B.; Ramey, M. B.; Reynolds, J. R. *Macromolecules* **1999**, *32*, 3970−3978.
(9) Yang, Y.; Pei, Q.; Heeger, A. J. *Synth. Met.* **1996**, *78*, 263−267.
(10) Baluschev, S.; Jacob, J.; Avlasevich, Y. S.; Keivanidis, P. E.; Miteva, T.; Yasuda, A.; Nelles, G.; Grimsdale, A. C.; Müllen, K.; Wegner, G. *Chemphyschem* **2005**, *6*, 1250−1253.
(11) Baluschev, S.; Keivanidis, P. E.; Wegner, G.; Jacob, J.; Grimsdale, A. C.; Müllen, K.; Miteva, T.; Yasuda, A.; Nelles, G. *Appl. Phys. Lett.* **2005**, *86*.
(12) Elsenbaumer, R. L.; Shacklette, L. W. In *Handbook of Conducting Polymers*; Skotheim, T. A., Ed.; Dekker: New York, 1986.
(13) Lamba, J. J. S.; Tour, J. M. *J. Am. Chem. Soc.* **1994**, *116*, 11723−11736.
(14) Rehahn, M.; Schlüter, A. D.; Wegner, G. *Makromol. Chem. Macromol. Chem., Phys.* **1990**, *191*, 1991−2003.
(15) Rehahn, M.; Schlüter, A. D.; Wegner, G.; Feast, W. J. *Polymer* **1989**, *30*, 1060−1062.
(16) Rehahn, M.; Schlüter, A. D.; Wegner, G.; Feast, W. J. *Polymer* **1989**, *30*, 1054−1059.
(17) Scherf, U. *J. Mater. Chem.* **1999**, *9*, 1853−1864.
(18) Chmil, K.; Scherf, U. *Acta Polym.* **1997**, *48*, 208−211.
(19) Kirstein, S.; Cohen, G.; Davidov, D.; Scherf, U.; Klapper, M.; Chmil, K.; Müllen, K. *Synth. Met.* **1995**, *69*, 415−418.
(20) Neher, D. *Macromol. Rapid Commun.* **2001**, *22*, 1366−1385.
(21) List, E. J. W.; Guentner, R.; de Freitas, P. S.; Scherf, U. *Adv. Mater.* **2002**, *14*, 374−378.
(22) Scherf, U.; List, E. J. W. *Adv. Mater.* **2002**, *14*, 477−487.
(23) Setayesh, S.; Marsitzky, D.; Müllen, K. *Macromolecules* **2000**, *33*, 2016−2020.
(24) Grimsdale, A. C.; Leclere, P.; Lazzaroni, R.; Mackenzie, J. D.; Murphy, C.; Setayesh, S.; Silva, C.; Friend, R. H.; Müllen, K. *Adv. Funct. Mater.* **2002**, *12*, 729−733.
(25) Büsing, A.; Heun, S.; Türk, S.; Leske, C. Patent WO2005104264, Nov. 3, 2005.
(26) Dams, R.; Malinowski, M.; Westdorp, I.; Geise, H. Y. *J. Org. Chem.* **1982**, *47*, 248−259.
(27) Jacob, J.; Sax, S.; Piok, T.; List, E. J. W.; Grimsdale, A. C.; Müllen, K. *J. Am. Chem. Soc.* **2004**, *126*, 6987−6995.
(28) See Supporting Information for further details.
(29) Zhang, Z. B.; Fujiki, M.; Tang, H. Z.; Motonaga, M.; Torimitsu, K. *Macromolecules* **2002**, *35*, 1988−1990.
(30) Hagberg, E. C.; Olson, D. A.; Sheares, V. V. *Macromolecules* **2004**, *37*, 4748−4754.
(31) Staab, H. A.; Bräunling, H. *Tetrahedron Lett.* **1965**, *6*, 45−49.
(32) Cervini, R.; Li, X. C.; Spencer, G. W. C.; Holmes, A. B.; Moratti, S. C.; Friend, R. H. *Synth. Met.* **1997**, *84*, 359−360.
(33) de Leeuw, D. M.; Simenon, M. M. J.; Brown, A. R.; Einerhand, R. E. F. *Synth. Met.* **1997**, *87*, 53−59.
(34) Grem, G.; Leditzky, G.; Ullrich, B.; Leising, G. *Synth. Met.* **1992**, *51*, 383−389.
(35) Cadby, A. J.; Lane, P. A.; Mellor, H.; Martin, S. J.; Grell, M.; Giebeler, C.; Bradley, D. D. C.; Wohlgenannt, M.; An, C.; Vardeny, Z. V. *Phys. Rev. B* **2000**, *62*, 15604−15609.
(36) List, E. J. W.; Partee, J.; Shinar, J.; Scherf, U.; Müllen, K.; Zojer, E.; Petritsch, K.; Leising, G.; Graupner, W. *Phys. Rev. B* **2000**, *61*, 10807−10814.
(37) Hsu, J. W. P.; Yan, M.; Jedju, T. M.; Rothberg, L. J.; Hsieh, B. R. *Phys. Rev. B* **1994**, *49*, 712−715.
(38) Leng, J. M.; Jeglinski, S.; Wei, X.; Benner, R. E.; Vardeny, Z. V.; Guo, F.; Mazumdar, S. *Phys. Rev. Lett.* **1994**, *72*, 156−159.

MA061007P